TRIMETHYLGUANOSINE SYNTHASE1 mutations decanalize female germline development in Arabidopsis

Lorena A. Siena[1] (iD), Caroline Michaud[2] (iD), Benjamin Selles[2] (iD), Juan Manuel Vega[1], Silvina C. Pessino[1] (iD), Mathieu Ingouff[2] (iD), Juan Pablo A. Ortiz[1] (iD) and Olivier Leblanc[2] (iD)

[1]Instituto de Investigaciones en Ciencias Agrarias de Rosario, CONICET-Universidad Nacional de Rosario, S2125ZAA, Zavalla, Argentina; [2]DIADE, Univ Montpellier, IRD, CIRAD, 34394, Montpellier, France

Summary

• Here, we report the characterization of a plant RNA methyltransferase, orthologous to yeast trimethylguanosine synthase1 (Tgs1p) and whose downregulation was associated with apomixis in *Paspalum* grasses.
• Using phylogenetic analyses and yeast complementation, we determined that land plant genomes all encode a conserved, specific TGS1 protein. Next, we studied the role of *TGS1* in female reproduction using reporter lines and loss-of-function mutants in *Arabidopsis thaliana*.
• *pAtTGS1:AtTGS1* reporters showed a dynamic expression pattern. They were highly active in the placenta and ovule primordia at emergence but, subsequently, showed weak signals in the nucellus. Although expressed throughout gametophyte development, activity became restricted to the female gamete and was also detected after fertilization during embryogenesis. TGS1 depletion altered the specification of the precursor cells that give rise to the female gametophytic generation and to the sporophyte, resulting in the formation of a functional aposporous-like lineage.
• Our results indicate that TGS1 participates in the mechanisms restricting cell fate acquisition to a single cell at critical transitions throughout the female reproductive lineage and, thus, expand our current knowledge of the mechanisms governing female reproductive fate in plants.

Introduction

In sexual organisms, meiosis and gametic union typically pattern life cycles into alternating diploid and haploid phases (Bowman *et al.*, 2016; Pandey *et al.*, 2022). In green algae and land plants, they consist in the sporophytic and gametophytic generations, each operating specific programs for establishing the reproductive lineages. During sporogenesis, diploid sporophytic cells are specified for meiosis and form male and female haploid spores, which in turn produce multicellular gametophytes that differentiate germ cells giving rise to the gametes. Finally, the union of a male gamete (sperm) and a female gamete (egg) produces a zygote, which is a new sporophyte. Some flowering plants reproduce through strategies that sidestep meiosis and gametic fusion but retain the typical alternating sporophytic-gametophytic ontogeny (Schmidt *et al.*, 2015). These behaviors, termed gametophytic apomixis (hereafter, apomixis), perpetuate for generations the maternal genotype, an appealing outcome for crop breeding (Ozias-Akins & Conner, 2020; Khanday & Sundaresan, 2021).

Although diverse, apomictic pathways all entail, first, the formation of functional, unreduced female gametophytes (FGs) from megaspore mother cells (MMCs) after meiosis bypass

(diplospory) or from nucellar cells surrounding the MMC (apospory) and, second, the parthenogenetic development of unreduced female gametes into maternal embryos. How these two processes operating in opposite directions (i.e. sporophyte-to-gametophyte and vice-versa) are established and coordinated remains poorly understood despite recent progress in deciphering the molecular differences between sexual reproduction and apomixis (León-Martínez & Vielle-Calzada, 2019; Barcaccia *et al.*, 2020; Schmidt, 2020). Each plant generation has evolved ways to prevent the developmental programs required to establish the other one (Mosquna *et al.*, 2009; Sakakibara *et al.*, 2013) and operates a specific reproductive developmental program, that is, the formation of spores (sporogenesis) and the formation of gametes (gametogenesis; Bowman *et al.*, 2016; Böwer & Schnittger, 2021; Dierschke *et al.*, 2021). Altered expression of these programs in time and space thus seems appealing for building apomictic life cycles (Schmidt *et al.*, 2015). However, although several regulatory factors for both generations were identified in sexual models (Nakajima, 2018; Hisanaga *et al.*, 2019; Pinto *et al.*, 2019; Lora *et al.*, 2019; Hater *et al.*, 2020; Khanday & Sundaresan, 2021; Kim *et al.*, 2021; Vigneau & Borg, 2021; Y. Li *et al.*, 2021; Cai *et al.*, 2022; Huang *et al.*, 2022; Petrella

et al., 2022; Sanchez-Vera *et al.*, 2022), no clear hookup with natural apomictic systems has emerged yet, except evidence for members of the RNA-directed DNA methylation pathway (Grimanelli, 2012; Selva *et al.*, 2017; Galla *et al.*, 2019). On the other hand, and contrary to inheritance studies suggesting a limited number of loci controlling apomixis, variation in the expression of large numbers of genes affecting a wide range of cellular activities usually differentiates sexual and apomictic developments (Brukhin & Baskar, 2019; Schmidt, 2020). Difficulties in accessing the cell types of interest have certainly hindered the deciphering of these changes and relevant orchestrating factors remain elusive thus far, except for a few candidates that remain functionally uncharacterized, for example, APOLLO (Corral *et al.*, 2013) and QUI-GON JINN (Mancini *et al.*, 2018). Moreover, deletion mapping in *Hieracium* apomicts identified two loci, LOSS OF APOMEIOSIS and LOSS OF PARTHENO-GENESIS (Koltunow *et al.*, 2011), whose action remains unresolved at the molecular level. Instead, comparative genomics in aposporous *Pennisetum squamulatum* and deletion mapping in diplosporous *Taraxacum officinale* identified two candidates encoding, respectively, a BABY BOOM-LIKE (BBML) transcription factor of the APETALA2 family and the PARTHENO-GENESIS (PAR) transcription factor (Conner *et al.*, 2015; Underwood *et al.*, 2022). Heterologous expression of these proteins in sexual relatives promotes the formation of parthenogenetic embryos that can give rise to viable maternal progenies (*Ps*BBML and *Oryza sativa* BBM homologs) and divisions in egg cells (*To*PAR), at least in species from their respective clades (Conner *et al.*, 2017; Khanday *et al.*, 2019; Underwood *et al.*, 2022).

In *Paspalum notatum* apomicts, we recently identified a candidate gene encoding a RNA methyltransferase with a *S*-adenosyl-L-methionine (SAM; pfam09445) domain typical of trimethylguanosine synthase1 (*TGS1*) in yeast (*Saccharomyces cerevisiae*) and animals (Siena *et al.*, 2014; Fig. 1a). In these organisms, transcription by RNA POLYMERASE II generates RNAs bearing a 7-methylguanosine (m^7G) 5′-end cap, whose conversion into $m^{2,2,7}G$-cap by TGS1 is essential for biogenesis and trafficking of several types of RNA molecules, including small nuclear and nucleolar RNAs (Mouaikel *et al.*, 2002; Hausmann *et al.*, 2008; Verheggen & Bertrand, 2012; Cheng *et al.*, 2020); quiescence-induced miRNAs (Martinez *et al.*, 2017); human telomerase RNAs (Chen *et al.*, 2020); heterochromatic noncoding RNAs involved in the establishment of centromeric heterochromatin (Yu *et al.*, 2021); and selenoprotein mRNAs (Wurth *et al.*, 2014). While Tgs1p in yeast consists in a SAM domain and a short N-tail harboring a nuclear localization sequence (NLS) region, animal TGS1 proteins have extended N-termini (Fig. 1a) embracing transcriptional regulation and other functions beyond RNA processing (Zhu *et al.*, 2001; Jia *et al.*, 2012). TGS1 mutations usually produce mild phenotypes related to mitosis and growth, including low temperature sensitivity in growing yeast (Mouaikel *et al.*, 2002); pericentromeric heterochromatin defects in *S. pombe* (Yu *et al.*, 2021); and reduced cell growth in mammals (Lemm *et al.*, 2006). In contrast, they compromise reproduction in budding yeast (no meiosis

commitment; Qiu *et al.*, 2011), *Drosophila* (germline and pupal altered development; Komonyi *et al.*, 2005; Cheng *et al.*, 2020), and mice (embryogenesis defects; Jia *et al.*, 2012).

In contrast to animals and yeast, little information is currently available for TGS1 function and contribution to plant developmental biology. Previous reports have shown a role in chilling resistance in *Arabidopsis thaliana* (Gao *et al.*, 2017) and flowering time in *Lupinus angustifolia* (Taylor *et al.*, 2021). In addition, *TGS1* expression levels and rates of residual sexuality in *P. notatum* apomicts were found to correlate positively (Siena *et al.*, 2014), an observation consistent with aposporous-like FGs formation in sexual *P. notatum* transformants expressing an antisense RNA-*PnTGS1* construct (Colono *et al.*, 2019). To gain further knowledge into the functional characterization of TGS1 proteins during plant reproduction, we first generated phylogenetic trees from plant TGS1 sequences and provide evidence for the conservation of a specific domain architecture across land plants. Next, by using reporter imaging and reverse genetics in *A. thaliana*, we demonstrated that the conserved TGS1 isoform is required for female germ cell specification and that loss-of-function causes phenotypes reminiscent of aposporous apomixis.

Materials and Methods

Plant materials

Arabidopsis thaliana (L.) Heynh seeds were stratified in the dark at 4°C for 2 d and then transferred to a growth chamber (22°C, long-day conditions). All crosses were performed using emasculated buds that we hand-pollinated 2 d after emasculation, unless stated otherwise. Ecotype Columbia (Col-0) was used as wild-type (WT) plants. T-DNA insertion lines for *AtTGS1* (*At1g45231*) were *tgs1-4* (SALK_020980) and *tgs1-5* (SALK_071682; see Supporting Information Fig. S1 for mutants' selection). Fluorescent reporter lines were used for female germline precursors (*pKNU:nlsYFP*; Payne *et al.*, 2004); synergid cells (*pNTA:nTdtomato*; Kong *et al.*, 2015); FG cell types using *FGR7.0* (Völz *et al.*, 2013) that contains *EC1:NLS_3xdsRed* (egg cell), *DD22:NLS_YFP* (central cell/endosperm), and *DD2:NLS_3xGFP* (synergid cells/endosperm); gametophytic cell fate and ploidy (*pWOX2-CENH3-GFP*; Keçeli *et al.*, 2017); and early embryo cell fate (*pS4:nGFP*; Kong *et al.*, 2015) and patterning (*pDRN : GFP*; Cole *et al.*, 2009). *tgs1* mutants containing these reporters were obtained from F2 plants, derived from crosses between *tgs1* mutants and the reporter lines, PCR genotyped to recover *tgs1* homozygous plants, and finally selected based on nonsegregating expression pattern of the reporter in ovules ($n > 50$). Observations reported here were performed using derivatives of one selected F_2 line per combination. For *pAtTGS1:AtTGS1-GFP* and *pAtTGS1:AtTGS1-GUS* reporter lines, we transformed Col-0 plants by floral dipping using binary vectors (see 'Molecular procedures' in the Materials and Methods section). T1 seeds were grown on solid Murashige & Skoog (MS) medium supplemented with BASTA (10 mg l^{-1}), hygromycin (30 mg l^{-1}), or kanamycin (50–200 mg l^{-1}) as selective markers. Germination tests were performed using two batches of 100

sterilized seeds per genotype that were sown onto germination medium (half MS salts supplemented with 1% agar) in Petri dishes and monitored for 10 d under a stereomicroscope. Developmental alterations in plantlets were screened under a stereomicroscope.

Phylogenetic reconstruction analyses

Sequences of green algae ($n = 12$) and land plants ($n = 59$) species were searched in public databases by BLASTp (eventually tBLASTn) using Tgs1p (*Saccharomyces* Genome Database ID:
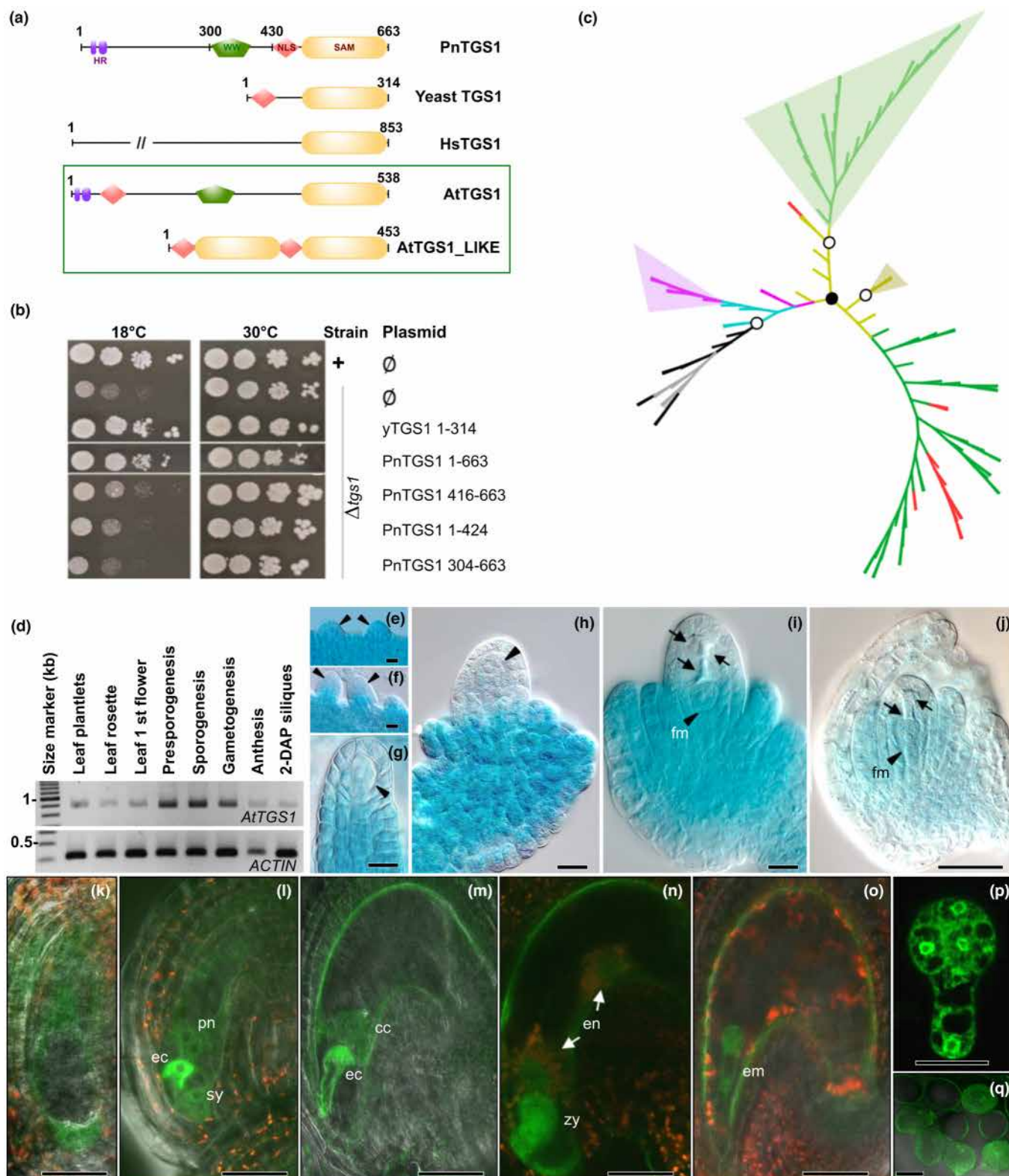
Fig. 1 Characterization of plant TGS1 proteins. (a) Scaled drawings of representative plant TGS1 methyltransferases. Note the unusual intragenic duplication of the SAM domain in AtTGS1-LIKE. HR, hydrophobic residues. At, *Arabidopsis thaliana*; Hs, *Homo sapiens*; Pn, *Paspalum notatum*. (b) Complementation in yeast Δ*tgs1* mutants expressing full-length and truncated PnTGS1 proteins growing at low (growth-sensitive) and high (growth-insensitive) temperatures. (+), wild-type (WT) strain BY4741. (c) Phylogenetic tree of Tgs1 orthologs in green lineages. Colored triangles show TGS1-LIKE monophyletic clades. Black and white dots indicate moderate branch support by the aBayes criterion: 0.5–0.75, and 0.75–0.9, respectively. All other nodes have values > 0.95. Black and gray: green algae encoding TGS1 proteins possessing and lacking a WW domain, respectively; blue, Bryophytes; pink, ferns; bronze, gymnosperms; green, angiosperms; red, land plant clades lacking TGS1-LIKE. (d) RT-PCR for *AtTGS1* and the *ACTIN11* control gene in *Arabidopsis* tissues. (e–j) GUS staining patterns in *pAtTGS1:AtTGS1-GUS* reporter lines showing accumulation in (e) placenta and ovule primordium (arrowheads); (f) young ovules (arrowheads) before MMC differentiation; (g) an ovule containing a MMC (arrowhead); (h) an ovule containing a mature MMC (arrowhead); and (i, j) postmeiosis ovules containing a surviving megaspore (arrowhead) and three degenerated spores (arrows). (k–q) Confocal images of *pAtTGS1:AtTGS1-GFP* reporter lines showing fluorescent signals in a four- (k) and an eight-nucleated (l) female gametophyte; a mature gametophyte (m); a zygote (n); a two-celled embryo (o); a 3-d after pollination (DAP) isolated globular embryo (p); and mature male gametophytes (q). Note the strong signal in the egg cell (l, m). cc, central cell; ec, egg cell; em, embryo; en, endosperm; fm, functional megaspore; pn, polar nuclei; zy, zygote. Bars: (g, h, q) 10 μm; (e, f, l–p) 30 μm.

SGD:S000006078; www.yeastgenome.org/) as a query. Amino acid sequences (Table S1) were first screened for known domains (e.g. SAM, WW, and NLS) using INTERPRO (https://www.ebi.ac.uk/interpro/search/sequence/) and MOTIFSCAN (https://myhits.isb-sib.ch/cgi-bin/motif_scan) and searched for conserved residues using the GenomeNet Bioinformatics Tools (https://www.genome.jp/tools/motif/MOTIF2.html). Phylogenetic analyses were performed using the Next Generation Phylogeny web service (https://ngphylogeny.fr) with the following workflow: MAFFT for multiple amino acid sequence alignments using a Blosum62 matrix and default parameters for gap extension and opening penalties; BMGE for alignment curation and selection of informative blocks using a Blosum62 matrix, a minimum block size of 5 and the default for remaining parameters; PhyML for tree inference (Blosum62 matrix; BEST option for tree topology search; aBayes criterion for branch support); and Newick default display for tree rendering.

Yeast procedures

Wild-type (BY4741) and Δ*tgs1* strains were transformed following the LiAc method (Gietz & Schiestl, 2007) using plasmids encoding full-length or truncated TGS1 proteins from *Paspalum notatum* Flüggé (see 'Molecular procedures' in the Materials and Methods section). Yeast cell lines were grown in liquid YPDA medium containing auxotrophic selecting markers (0.2% Ura, 2% Met and 1% Leu) for 24 h at 30°C under shaking. For functional complementation, cells were harvested by centrifugation (1200 *g*, 5 min), resuspended into sterile water to $OD_{600} = 0.5$, and sequentially diluted 10, 100 and 1000 times in sterile water. Ten μl of each dilution was spotted onto agar medium supplemented with 0.5% glucose and the auxotrophic selecting markers and incubated 4 d at 30°C or 9 d at 18°C before scoring. Yeast strains, BY4741 (MATa; ura3Δ0; leu2Δ0; his3Δ1; met15Δ0) and Δ*tgs1* (BY4741; MATa; ura3Δ0; leu2Δ0; his3Δ1; met15Δ0; YPL157w::kanMX4), were obtained at http://www.euroscarf.de.

Molecular procedures

For T-DNA insertion line genotyping, genomic DNA extracted from leaf tissue was assayed by PCR. For RT-PCR

analyses, RNA was isolated using TRIZOL (Invitrogen) and treated with DNAseI. Leaves collected at three developmental stages (plantlets, rosette, and flowering onset) and floral buds collected from presporogenesis to 2 d after pollination were used as samples for vegetative and reproductive tissues, respectively (three WT and *tgs1* plants/sample). Following reverse transcription using 1 μg of total RNA and Invitrogen Super-Script III Reverse Transcriptase according to manufacturer's instructions, cDNAs were amplified for *AtTGS1* and *ACTIN11* as a control for constitutive expression. To generate constructs reporting AtTGS1 expression, we ordered from GenScript USA Inc. a pUC57-KAN vector containing a synthesized DNA fragment spanning 1732 base pairs (bp) upstream of the initiation codon up to the last amino acid before the stop codon of *AtTGS1* (4912 bp) and flanked by the attL Gateway sites. This vector was used as an entry clone in LR reactions (Invitrogen) with two Gateway destination vectors, pGWB604 and pGWB433, to produce *pAtTGS1:AtTGS1-GFP* and *pAtTGS1:AtTGS1-GUS*, respectively. For yeast expression vectors, coding sequences were amplified from cDNA with specific primers and directionally cloned into the pENTR/D-TOPO entry vector (Invitrogen). Entry plasmids were recombined (LR clonase II, Invitrogen) with destination vectors pRS423-GPD-ccdb-EGFP (AddGene #14198) and pRS426-GPD-ccdb-DsRed (AddGene #14372) for monitoring the expression of PnTGS1 and Tgs1p, respectively. All primers are shown in Table S2.

Whole-mount preparations and microscopy

Pollen grains were collected from open flowers, placed under a coverslip in sterile water containing 1 μg ml^{-1} DAPI (4′,6-diamidino-2-phenylindole) for 5 min. Ovule clearing and histochemical detection of the *uidA* reporter gene product were performed as described previously (Autran *et al.*, 2011). Callose detection in ovules stained with aniline blue was performed as described previously (Cao *et al.*, 2018). Observations were made on either a Zeiss Axio Imager or a Leica DM2500 under Differential Interference Contrast (DIC) optics for cleared ovules. Fluorescence in ovules mounted in 30% glycerol was imaged on a Zeiss Axio Imager using a 450–490 nm excitation filter and a BP 525/

50 nm bandpass filter. For *pAtTGS1:AtTGS1-GFP* and *pWOX2-CenH3-GFP* signals, imaging was also performed using a confocal microscope (Leica TCS SP8 and Zeiss LSM880 Airyscan).

Flow cytometry

Cell ploidy in bulks containing four mature seeds of WT or *tgs1* plants was determined by estimating nuclear DNA content using a flow cytometry procedure adapted from Matzk *et al.* (2000). Seeds were placed in a glass Petri dish into a 50-µl drop of extraction buffer (Tween20 0.5%, citric acid 0.1 M) and grinded using a glass pestle. After collecting the remains by rinsing the pestle with 150 µl of sodium phosphate monobasic 0.4 M, the extracts were filtered (30-µm mesh) and the nuclei solution was supplemented with 4 µl of Ribonuclease A (0.5 mg ml^{-1}). After incubation at room temperature for 5–10 min, 10 µl of 1 mg ml^{-1} Propidium iodide (Sigma, P4170) was added to the solution and DNA contents were measured using a Becton-Dickinson FACSAria™ II workstation with excitation and emission wavelengths of 538 and 617 nm, respectively. We used FlowJo v.10.0.7 (BD Biosciences, Wokingham, UK) for data analysis (at least 2500 nuclei/scoring window, except for samples with low nuclei concentration) and graphical views. The null hypothesis that the proportions of nuclei corresponding to three DNA content classes (2×, 3×, >3×) obtained from each *tgs1* bulk were similar to that estimated from 17 bulks of WT seed was tested using Pearson's chi-squared tests. When rejected, significant increase in 3× nuclei compared with 2× nuclei was assessed using chi-squared tests.

Results

TGS1 plant sequences and phylogenetic relationships

Previous works showed that a single gene encodes TGS1 in all eukaryotes, but *Arabidopsis* and rice possess two copies (Fig. 1a; Mouaikel *et al.*, 2002, 2003). Since *TGS1* family members have remained largely uncharacterized in the green lineage, we first showed by successful complementation in Δ*tgs1* yeast that the product encoded by the *Paspalum TGS1* candidate gene for apomixis is a functional homolog of Tgs1p (Fig. 1b). Next, we performed phylogenetic analyses using protein sequences retrieved by BLASTP searches from sequenced genomes of Chlorophytes (green algae; *n* = 12) and Streptophytes, including 57 land plant species and two of their Charophytes (freshwater algae) ancestor species (Table S1). As suggested in *Arabidopsis* (Gao *et al.*, 2017), sequences alignment first revealed highly conserved C-termini harboring a nuclear localization sequence (NLS) adjacent to the SAM domain, while N-tails varied in length and domain composition depending on the presence of a protein-interacting WW domain (Sudol, 1996) and two stretches of conserved residues (>75% identity) with a hydrophobic pattern (LMKEMNDLGLPVSF and AIRALGHLFRLKEVFLEDD for *A. thaliana*; hydrophobic residues are underlined; Figs 1a, S2; Notes S1). BLASTP searches using the consensus sequence of these hydrophobic patterns produced no hit outside of the Viridiplantae. Although their function remains speculative, hydrophobic residues participate in

stabilization of protein structure and complexes. Interestingly, and contrary to the WW domain that is dispensable for complementing Δ*tgs1* yeast strains (Gao *et al.*, 2017), our data suggest that complementation in Δ*tgs1* yeast requires at least one of these two motifs, as N-terminally truncated PnTGS1 containing the WW domain, the NLS and the SAM domain were unable to rescue Δ*tgs1* strains (Fig. 1b).

Phylogenetic reconstruction using conserved blocks from alignments recapitulated green plants phylogenomics (One Thousand Plant Transcriptomes Initiative, 2019; Figs 1c, S3; Notes S2). Unsurprisingly considering the many questions persisting on their relationships and evolution, we obtained a poor resolution among the Chlorophytes algae sequences used here. Nevertheless, all species possess a single gene encoding a protein that contains a potentially catalytically active SAM domain, but highly variable N-tails regarding length and conserved motifs composition. In contrast, phylogenetic resolution in Streptophytes first identified a TGS1 ortholog in land plants, whose core components (hydrophobic residues; WW, NLS, and SAM domains; Fig. 1a) were conserved since they diverged from the Charophytes lineage. Furthermore, three monophyletic clades, clustering paralogs with large N-tail truncations lacking the WW domain, can be distinguished at different evolutionary times, indicative of distinct ancient duplication events followed by significative structural rearrangements in ancestors of ferns, Gymnosperms and Angiosperms. Accordingly, we followed Gao *et al.* (2017) nomenclature adopting *TGS1* for the genes encoding the conserved WW-SAM protein and *TGS1-LIKE* for the paralogous genes. Finally, sporadic duplications eventually followed by rearrangements (e.g. incomplete intragenic duplication in *A. thaliana TGS1-LIKE*; *TGS1* duplication in *Glycine max* followed by N-tail truncation) and frequent losses of acquired paralogs in extant clades (families or species) of phylogenetic trees complete TGS1s evolutionary trajectory in plants (Figs 1a, S3). While TGS1-LIKE paralogs appear dispensable, the retention of a single, highly conserved architecture in TGS1 proteins suggests that they fulfill essential functions in plants.

TGS1 expression during female reproductive development

Our previous analyses of *TGS1* expression and depletion in *P. notatum* ovules (Siena *et al.*, 2014; Colono *et al.*, 2019) and the phylogeny reconstruction previously reported prompted us to further decipher the function of TGS1 using the plant model *A. thaliana*. First, RT-PCR experiments revealed higher *TGS1* transcripts accumulation in reproductive organs compared with vegetative tissues (Fig. 1d). Next, to precisely monitor protein accumulation, we generated *pAtTGS1:AtTGS1-GUS/GFP* reporter lines to express C-terminal translational fusions of TGS1 to the beta-glucuronidase or the GFP protein, respectively. Reporter expression analyses for both constructs (at least three independent transformants each and *n* > 100 ovules per stage) agreed with RT-PCR experiments (Figs 1e–q, S4). Signal accumulated to high amounts in cells of the placenta, the sporophytic tissue that differentiates the ovules, and in those of emerging ovule primordia (Figs 1e, S4a). As ovules grew, staining intensity decreased along the proximal-distal axis and,

before meiosis initiated, the L1 cell layer and the nucellus, including the MMC, showed a weak, patchy expression (Figs 1f–h, S4b). These two contrasting expression domains persisted after meiosis but, in contrast to the MMC and the degenerating spores of the tetrad, the surviving functional megaspore (FM) stained intensely and was embedded in the proximal AtTGS1 expression domain (Fig. 1i). This pattern in subcellular localization might also indicate differences in activity as reported in yeast and humans, where Tgs1 can exist as two species with different substrate and localization specificities (Verheggen & Bertrand, 2012). The FM then produces through three mitoses a coenocyte that differentiates into a mature, seven-celled female gametophyte (FG) typically containing: three antipodal cells; two synergid cells (SCs); and two gametes, the haploid egg cell and the dihaploid central cell (Hater *et al.*, 2020). We observed diffuse, fading into background signals within developing coenocytic gametophytes and surrounding maternal tissues (Figs 1j, k, S4c). During nuclear migration, but before cellularization and differentiation occurred within FGs, the signal increased in the precursor nucleus of the egg cell (Fig. 1l) and, at maturity, it became restricted to gametic cells, being more intense in the egg (Fig. 1m). Mature male gametophytes showed a similar pattern, with diffuse signals in the generative cell and bright intensities in sperm cells (Fig. 1q). Finally, during early seed development (1–3 d after fertilization), signal accumulated essentially in the zygote (Figs 1n, S4d,e) and the developing embryo (Figs 1o,p, S4f–j) regardless of reporter inheritance, therefore suggesting early activation of the paternal allele (Fig. S4d–j). Note that no signal was detected throughout endosperm development, except for faint staining at early developmental stages (up to three rounds of nuclear divisions; Fig. 1n), suggesting maternal carryover from the central cell rather than transcriptional activity.

TGS1 restricts female germline specification

The peculiar domain organization of TGS1 in plants and its expression pattern in developing ovules suggest a preponderant role during plant reproduction. To test this hypothesis, we further characterized two *Arabidopsis* T-DNA insertion lines carrying *tgs1* loss-of-function alleles, SALK_020980 (*tgs1-4*) and SALK_071682 (*tgs1-5*; see Fig. S1a,b for details). High proportions of aborted seeds in *tgs1* heterozygous and homozygous plants (Fig. S1c,e) and segregation against *tgs1* mutants in progenies of heterozygous plants (Table 1) suggested defects in gametogenesis or embryogenesis. Indeed, reciprocal crosses between WT and *tgs1*/+ plants revealed reduced maternal transmission of *tgs1* alleles (Table 1). Finally, in crosses between *tgs1-4* mutants heterozygous for *pAtTGS1:AtTGS1-GUS* and WT plants, gametes carrying the GUS construct were significantly more transmitted (χ^2 (1, $n = 89$) = 4.05, $P < 0.05$; Table 1) as observed for the WT allele in progenies derived from *tgs1*/+ × WT crosses. This suggested that our constructs are fully functional.

Since *tgs1* pollen development showed no visible defects when stained using DAPI (> 95% of tricellular pollen grains in three individuals for each mutant line; Fig. S1d), we investigated ovules using differential interference contrast (DIC) microscopy and fluorescent protein reporters (Fig. 2). Before meiosis, most WT ovules (95%, $n = 400$) differentiated a single MMC (Fig. 2a) while the remaining ones had two, sporadically three, cells resembling MMC, that is, also exhibiting enlarged size and nucleus compared with surrounding cells. In contrast, *tgs1-4* and *tgs1-5* ovules exhibited one extra enlarged cell at significantly higher proportions than WT ovules (two-tailed P value for Fisher's exact test < 0.0001; Fig. 2c,d), respectively: 16% ($n = 183$) and, 18% ($n = 150$). Furthermore, *tgs1-4* ovules exhibited two extra enlarged cells at a frequency of 2% ($n = 183$; Fig. 2d). To explore whether the enlarged cells had MMC identity, we analyzed *tgs1-4* plants expressing *pKNU:nlsYFP*, a preferential marker of MMCs also detected in megaspores of WT ovules (Payne *et al.*, 2004; Fig. 2b,f,h). In *tgs1-4* ovules containing multiple enlarged cells, we found that *pKNU* was active in only one of them, suggesting only one is specified for meiosis (Fig. 2e,g).

Next, observations during meiosis revealed that WT ($n = 95$) and mutant ($n = 109$) ovules contained the meiotic products of a single tetrad (Fig. 2h–n). *pKNU:nlsYFP* signal was restricted to the chalazal spore in most WT ovules ($n = 93$; Fig. 2h) while 12 *tgs1-4* degenerating tetrads (11%) had two fluorescent chalazal spores (Fig. 2i). Callose is a typical marker of meiosis, which

Table 1 Transmission of *tgs1* alleles in *Arabidopsis thaliana*.

Crosses	Progeny genotypes			Expected ratio	χ^2
	Tgs1/Tgs1	*Tgs1/tgs1*	*tgs1/tgs1*		
tgs1-4/Tgs1 × *tgs1-4/Tgs1*	73	77	33	1 : 2 : 1	22.07***
tgs1-5/Tgs1 × *tgs1-5//Tgs1*	45	47	20	1 : 2 : 1	17.03***
tgs1-4/Tgs1 × Col-0	106	52	–	1 : 1	18.45***
Col-0 × *tgs1-4/Tgs1*	97	111	–	1 : 1	0.94[ns]
tgs1-5/Tgs1 × Col-0	77	39	–	1 : 1	12.44***
Col-0 × *tgs1-5/Tgs1*	32	30	–	1 : 1	0.06[ns]
	Tgs1/tgs1-4[GUS]	*Tgs1/tgs1-4*			
tgs1-4/tgs1-4:GUS/- × Col-0 Col-0 ×	54	35	–	1 : 1	4.05**
tgs1-4/tgs1-4:GUS/-	44	48	–	1 : 1	0.10[ns]

Col-0 was used as wild-type (WT). χ^2, statistic value of two-sided χ^2 tests indicating nonsignificant (ns) and significant deviation from the expected ratio (**, $P < 0.05$; ***, $P < 0.001$). GUS: *pAtTGS1:AtTGS1-GUS*; *tgs1-4*[GUS]: complementation of *tgs1-4* by GUS.
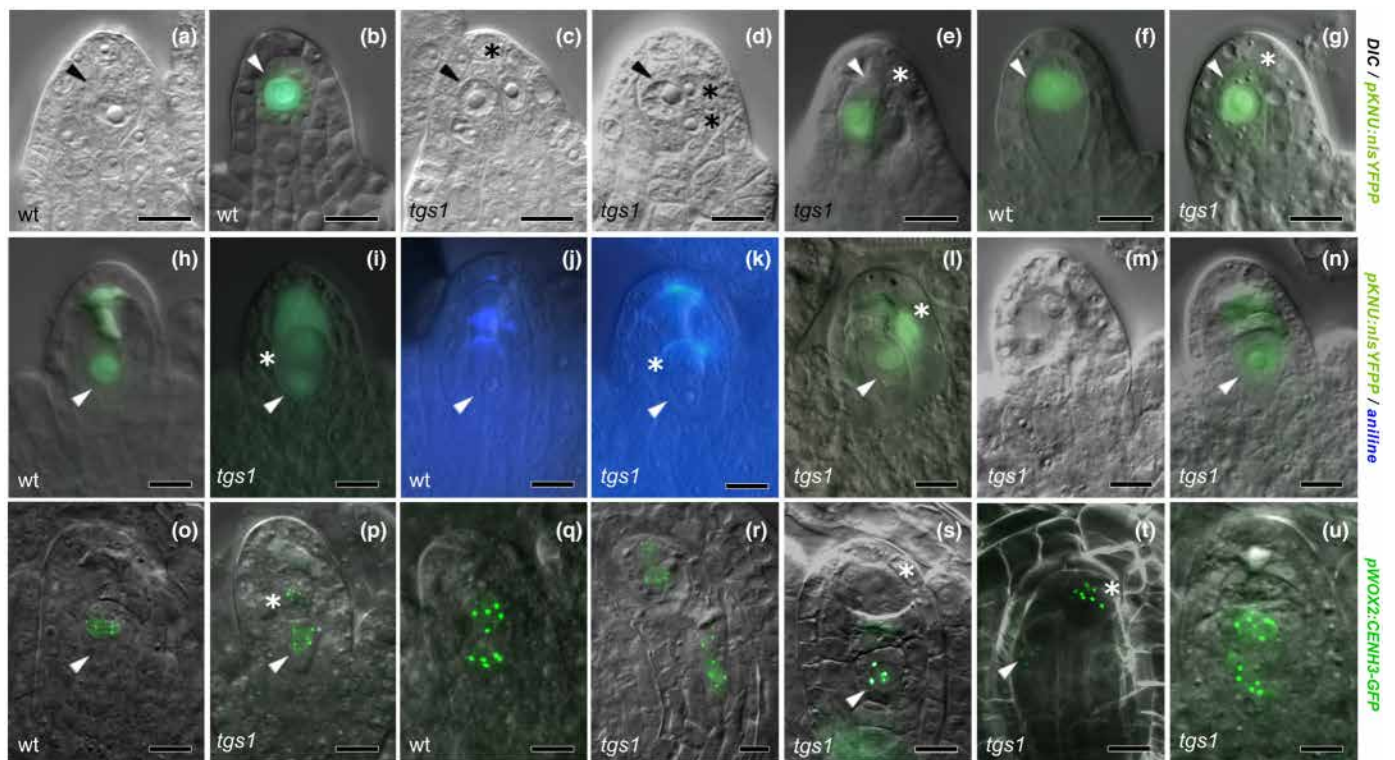
Fig. 2 TGS1 depletion triggers additional female germline in *Arabidopsis thaliana*. Ovule development in wild-type (WT) and *tgs1* plants carrying *pKNU:nlsYFP* (a–n) and *pWOX2-CENH3-GFP* (o–u). (a–g) Premeiotic ovules containing (a–e) enlarging MMCs (arrowhead) and (f, g) mature MMCs (arrowhead) accompanied by MMC-like enlarged cells (asterisks) in *tgs1* ovules. (h–u) Early steps of gametophytic development in WT ovules showing a single tetrad with one surviving megaspore (h, j, o) and a binucleated FG (q). Note the reminiscent signal of *pKNU:nlsYFP* and the strong dotted signal of *pWOX2-CENH3-GFP* indicating reduced FM. In contrast, *tgs1* ovules at meiosis showed several phenotypes, including tetrads with two FM (i, k, p) resulting in multiple reduced, binucleated FGs (r); *pKNU:nlsYFP* and *pWOX2-CENH3-GFP* ectopic signal in enlarged MMC-like cells near the FM (l, t) resulting in the development of unreduced binucleated FGs (m, n, u); and extremely enlarged MMC-like cells lacking *pWOX2-CENH3-GFP* signal near a correctly specified, reduced FM (s). Note that (m, n) show different optical plans of the same ovule (see also Supporting Information Fig. S5), containing a binucleate FG (m) and a tetrad of megaspores (n). Fluorescence signals detected for reporters and callose were merged with DIC images in (b, e–i, l, n–u) and (j, k), respectively. Arrowheads indicate the legitimate female germline cells initiating megasporogenesis (premeiotic ovules) and gametophyte development, while asterix indicates candidate precursors for additional female germline development. Bars, 10 μm.

starts depositing in MMC cell walls and shows high accumulation in dyads and tetrads, while it quickly disappears around the surviving FM (Webb & Gunning, 1990). Interestingly, callose patterns revealed by aniline blue staining showed no deposition in the walls between the two chalazal spores (7/50 tetrads in *tgs1* ovules; Fig. 2k). Note that this pattern was not detected in WT tetrads where callose typically deposited around the three micropylar spores (Fig. 2j).

At later stages of meiosis, in ovules containing extra MMC-like cells, *pKNU:nlsYFP* signal appeared fading in the surviving megaspores of the tetrad while strong expression was detected in the enlarged nucleus of most MMC-like cells ($n = 7$ out of 8 ovules; Fig. 2l). Finally, in five ovules, we could observe a binucleated embryo sac lacking KNU expression and adjacent to the legitimate tetrad (Figs 2m,n, S5). Therefore, while meiosis occurs in the specified MMC, MMC-like cells in TGS1-deficient ovules retain a potential for germline specification that expresses during the late stages of meiosis. These results suggest that KNU repression by TGS1 in nucellar cells surrounding the MMC contributes to confining female germline specification to a single cell.

TGS1 loss-of-function relaxes control of gametophytic and gametic developments

Adoption of gametophytic program was assessed using the *pWOX2-CENH3-GFP* reporter (Keçeli *et al.*, 2017). While only FM and FG nuclei were labeled in WT ovules throughout gametophytic development (Figs 2o,q, 3d), we detected signals in all additional surviving spores of *tgs1* tetrads ($n = 26$; Figs 2p, S6a) and in all but a few MMC-like cells adjacent to a FM ($n = 5$; Fig. 2t) among 105 ovules. These observations indicate that *tgs1* mutations can promote ectopic gametophyte formation in both somatic nucellar cells and tetrad meiotic products, therefore suggesting that in *Arabidopsis* TGS1 acts to restrict the number of cells committed to form a FG both within and outside of the canonical lineage. In support, we observed in ovules at early gametogenesis ($n = 86$): a single reduced, binucleated FG along with one additional surviving spore ($n = 10$; Fig. S6d); two reduced, binucleated FGs ($n = 5$; Figs 2r, S6g); and one unreduced binucleated FG ($n = 2$; Figs 2u, S6e), indicating that both types of spores (i.e. reduced and unreduced) are likely functional.
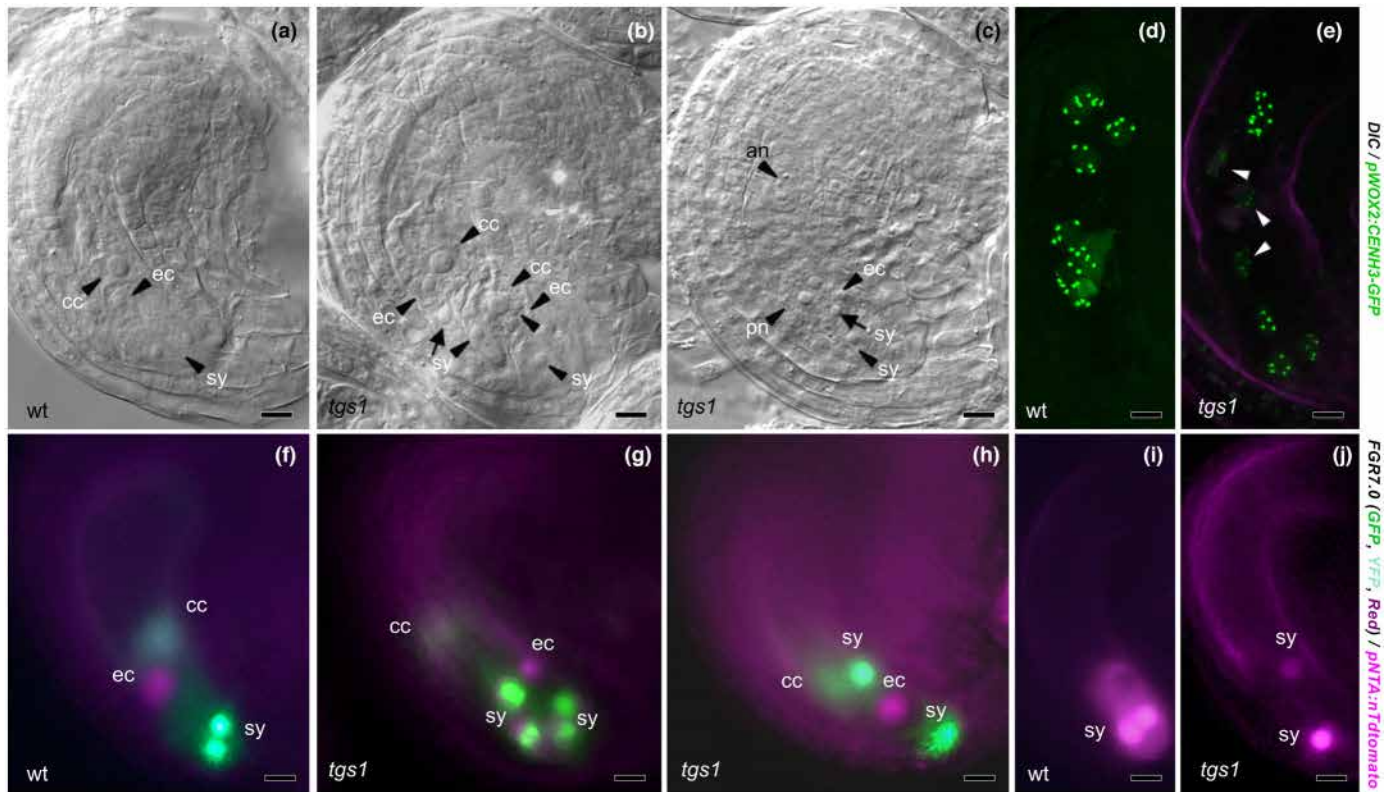
Fig. 3 TGS1 depletion causes multiple gametophytic and gametic developments in *Arabidopsis thaliana*. DIC observations (a–c) and signals from fluorescent reporters (d–j) in WT and *tgs1* ovules at anthesis. Wild-type (WT) ovules (a, d, f, i) typically contain one eight-nucleated, seven-celled FG composed of three antipodal cells (an) at the chalazal end; a central cell (cc) which polar nuclei have fused; and one egg cell (ec) and two synergid cells (sy) at the micropylar end. Most common defects observed in mutant ovules were: (b) multiple FGs; abnormal number of nuclei in the central region (e) and the micopylar region (g); alterations in synergid cells position (c, h, j); and mixed identity in the egg apparatus (g, h; see also Supporting Information Fig. S7). Confocal projections in (d, e) were obtained from *pWOX2-CNH3-GFP* ovules and epi-fluorescence signals in (f–h) and (i, j) from *FGR7.0* (ec: *EC1::NLS_3xdsRed*; sy: *DD2::NLS_3xGFP*; cc: *DD22::NLS_YFP*) and *pNTA:nTdtomato* ovules, respectively. Bars, 10 μm.

Finally, our observations support the hypothesis that extra MMC ectopically express both *pKNU:nlsYFP* and *pWOX2-CENH3-GFP*.

At later stages of gametogenesis, while WT mature ovules always contained a typical seven-celled FG ($n > 200$), we observed in *tgs1-4* and *tgs1-5* cleared ovules ($n = 116$ and $n = 100$, respectively) multiple FGs (6.5%) as well as FGs affected in nuclei number or positioning (15%; Fig. 3a–c). These phenotypes were further characterized in *tgs1* lines carrying *pWOX2-CENH3-GFP*, which revealed mature FGs with extra nuclei (Fig. 3d,e), and fluorescent reporters for gametic (*FGR7.0*) and SC fates (*FRG7.0*; *pNTA:nTdtomato*). Using *FGR7.0* ($n = 111$), gametic cells usually exhibited the WT phenotype (Fig. 3f) whereas SCs showed doubling, likely after an extra division (2.3%; Figs 3g, S7a,b); altered positioning (9.2%; Fig. 3h, S7c,d); and egg cell marker ectopic expression (31.1%; Fig. S7a,b). Such alterations were never observed in WT FGs ($n > 200$). The gametic potential in SCs in *tgs1* was confirmed by observations using *pNTA:nTdtomato* in *tgs1* FGs (Fig. 3i,j). Furthermore, cell fate determination in the egg apparatus of *tgs1* FGs seemed uncoupled from nucleus positioning since identity was maintained in SCs found at abnormal positions and, reciprocally, acquisition of egg cell identity occurred in correctly positioned

SCs (Figs 3, S7). Nevertheless, most FGs exhibited at least one properly specified SC according to *FRG7.0* and *pNTA* expression at the micropylar end, therefore suggesting that *tgs1* FG can mediate pollen tube attraction and sperm delivery.

tgs1 seeds show defects in both fertilization products

Examination of fertilized *tgs1* ovules in plants revealed defects in the endosperm, the embryo or both. First, we observed seeds 2–4 d after pollination (DAP) lacking endosperm or containing an abnormal endosperm with few enlarged nuclei (15 and 5 out of 161 *tgs1-4* seeds and 6 and 4 out of 167 *tgs1-5* seeds, respectively; Fig. 4a–e). Cell fate reporter analysis in 1–3 DAP *tgs1* seeds further revealed abnormal identity in endosperm nuclei as ectopic signal for embryo-specific *pS4:nGFP* reporter was detected (12/58 and 16/136 in *tgs1-4* and *tgs1-5* ovules, respectively; Fig. 4f–m), while both endosperm reporters in *FGR7.0* (i.e. *DD22::NLS_YFP* and *DD2::NLS_3xGFP*) showed the expected signal in endosperm nuclei of most ovules (86/91 and 31/33 in *tgs1-4* and *tgs1-5* ovules, respectively; Fig. 4n–q). Interestingly, ectopic expression of *FGR7.0* endosperm reporters was detected in *tgs1* embryos at 2 DAP (15/39 and 8/40 in *tgs1-4* and *tgs1-5* ovules, respectively; Fig. 4o–q). Therefore, the ectopic signals generated
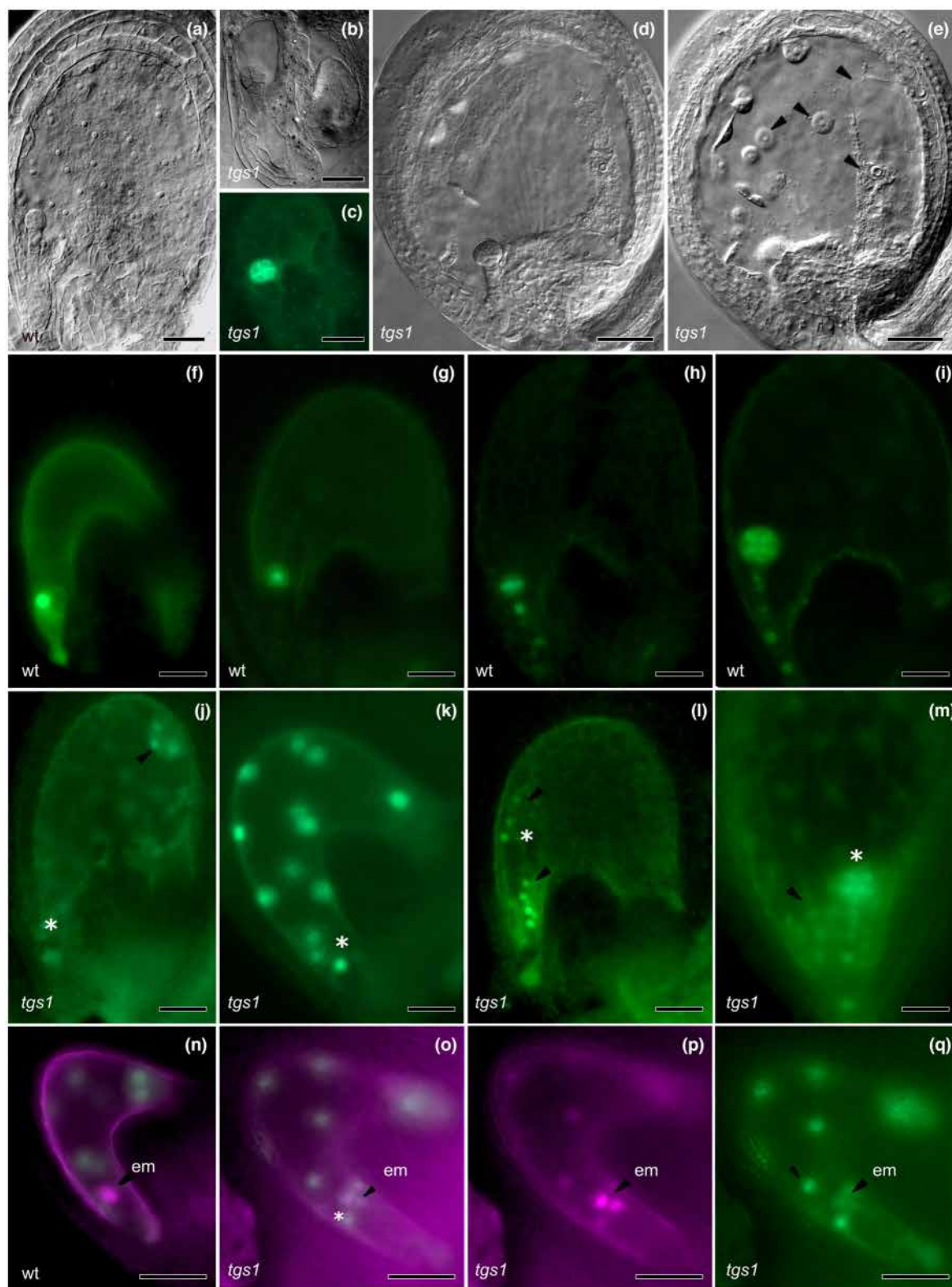
Fig. 4 Developmental effects in *tgs1* seeds of *Arabidopsis thaliana*. (a) Wild-type (WT) ovule showing normal endosperm development at 2 d after pollination (DAP). (b, c) DIC image (b) and *pDRN:GFP* expression (c) in an aborted *tgs1-4* seed containing a wt, globular embryo and lacking endosperm. (d, e) Two different optical plans of the same 2-DAP seed containing a globular embryo (d) and abnormal endosperm nuclei (arrowheads). (f–m) Specific expression of *pS4:nGFP* in a zygote (f) and developing embryos (g–i) in WT seed compared with *pS4:nGFP* ectopic expression in endosperm nuclei (arrowheads) of *tgs1-5* seeds (j–m). The embryo is indicated by an asterisk. (n) WT seed showing specific expression of *pEC1:NLS_3xdsRed* (magenta) in a two-celled embryo (arrowhead) and of *DD2:NLS_3xGFP* (green) in endosperm nuclei. (o–q) *FGR7.0/tgs1-4* seed with an embryo (arrowhead) exhibiting mixed identities (o, merged signals; p, *pEC1:NLS_3xdsRed* signal; q, *DD2:NLS_3xGFP*). Bars: (b, c) 10 μm; (f–q) 30 μm; (a, d, e) 50 μm.

by *pS4:nGFP* and *FGR7.0* suggest that both fertilization products suffer from mixed identities in a significant number of *tgs1* ovules. Furthermore, DIC observations and fluorescence analysis for two embryo cell fate reporters, *pS4:nGFP* and *pDRN:GFP*, indicated that loss of apical-basal polarity (Fig. 5a–e) and aberrant cell division patterns in both proper embryos (Fig. 5g–n) and suspensors (Fig. 5f,o,p) were significantly more common at 2–5 DAP in *tgs1* embryos (27/380 and 29/468 in *tgs1-4* and *tgs1-*
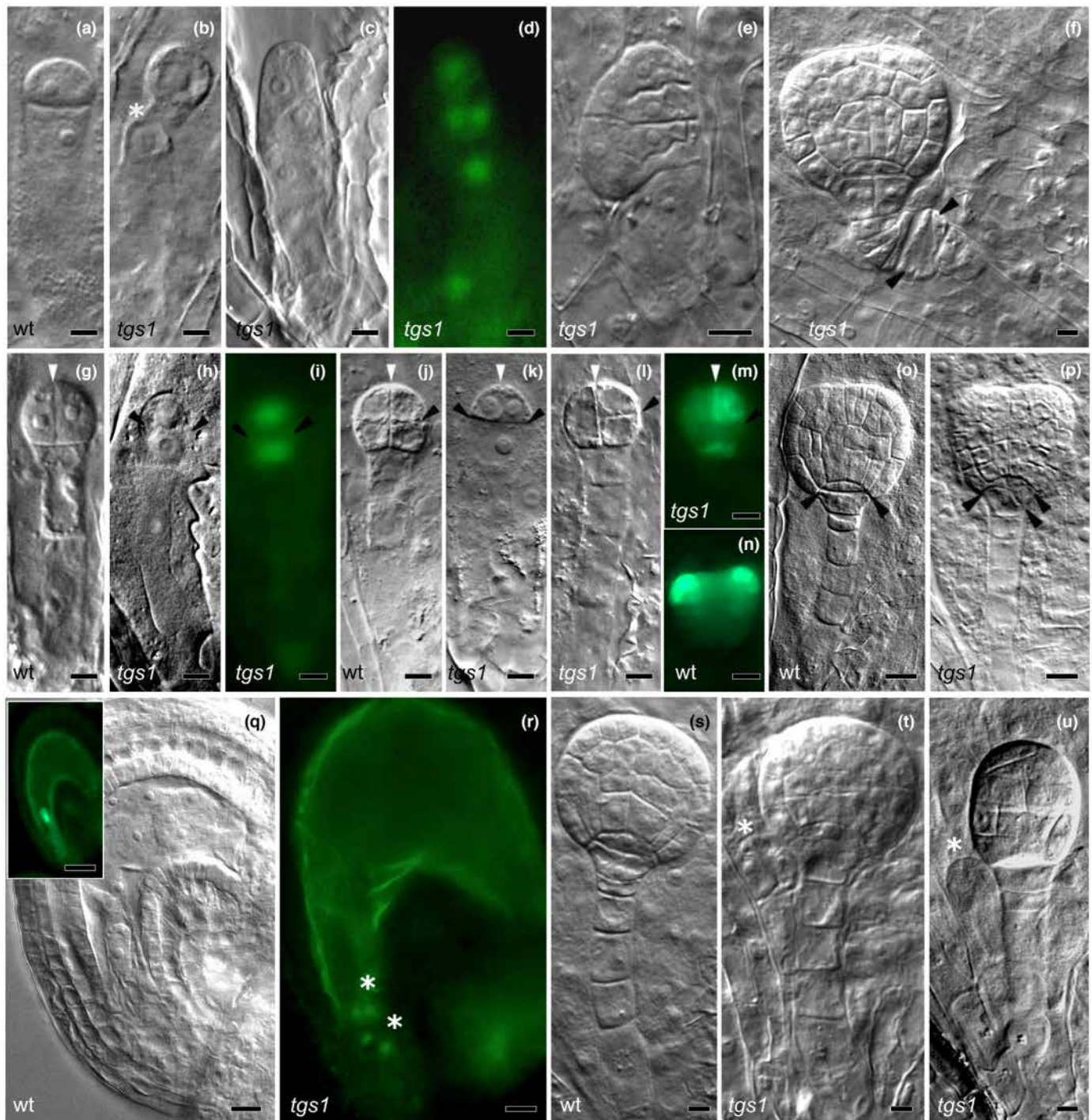

Fig. 5 Embryogenesis in wild-type (WT) and *tgs1* plants of *Arabidopsis thaliana*. (a–p) Alterations in cell identity and division patterns include loss of apical-basal polarity and fate specification resulting in the formation of extra embryo in the suspensor (b), filamentous embryonic structures (c, d), disorganized embryo (e) and disordered divisions affecting lower suspensor cells (f) and hypophysis cell (o, p). (d) shows *pS4:nGFP* expression. (g–n) Normal (g, j, n) and disordered divisions (arrowheads) in the apical cell (h, i) and daughter cells (k–m), associated occasionally with mislocalization of the *pDRN:GFP* cell identity marker (m, n). (i) shows *pS4:nGFP* expression. (q–u) Formation of extra zygotes (r; *pS4:nGFP* expression) and extra embryos (t, u). Stars indicate supernumerary embryos. Inset in (q) shows *pS4:nGFP* expression. Bars, 5 μm.

5 seeds, respectively) than in WT embryos observed at the same stage (3/233; two-tailed *P* value for Fisher's exact test < 0.0005). More strikingly, while WT fertilized ovules always contained a single embryo (*n* > 500), we observed the formation of two zygotes (4/100) and multiple embryos (14/409) during early (Fig. 5q–u) and late (Fig. S8a) *tgs1* seed development. When sown on germination medium, and consistently with our observations indicating altered embryo patterning, only 67% of mutant (*tgs1-4* and *tgs1-5*) seeds germinated (*n* = 400; WT germination > 95%, *n* > 200; Fig. S8). Out of these, 20% and 29% exhibited defects in primary root and leaf, respectively (developmental defects in WT < 2%; *n* > 200; Fig. S8). Finally, our observations in *tgs1* germinated seeds indicated the generation of suspensor-derived twin embryos (3.1%; Fig. S8b,g). However, we found no evidence for multiple dizygotic embryos, suggesting that only one of the embryos detected during early and late seed development is able to complete development.

tgs1 seeds contain triploid embryos

As our observations suggested that mature, unreduced FG occur at low frequency, we asked whether these FG are functional, that is, do *tgs1* seeds contain unreduced embryos? We thus determined DNA contents in nuclei from mature seeds by flow cytometry. In *A. thaliana*, nuclei typically distribute among peaks generated by embryo cells (2× and 4×) and cells of the remanent endosperm (3× and 6×) while maternal tissues from the seed coat contain no intact nuclei (Matzk *et al.*, 2000). As *pWOX2:CENH3-GFP* sperm nuclei at anthesis showed a five-dot pattern corresponding to the reduced number of chromosomes (Fig. S6h,i), seeds successfully formed from an unreduced, female FG therefore are expected to contain a 3× embryo. First, we characterized nuclei distribution in 17 bulks of four WT seeds, which showed peaks corresponding to 2×, 3×, and > 3× DNA content values (61%, 8% and 31%, respectively; Fig. 6a,d). This indicated that all WT seeds contained a diploid embryo and a small proportion of 3× cells likely from remanent endosperm. The same procedure applied for screening 300 *tgs1-4* seeds and 220 *tgs1-5* seeds (respectively, 75 and 55 bulks) allowed the detection of five bulks showing a significant difference in nuclei proportions compared with estimated mean DNA content values in bulks of WT seeds. Out of these, an increased proportion in 3× cells explained this difference, while the remaining bulk contained a higher proportion of cells with > 3× DNA content value (Fig. 6b–d). Our procedure allowed the detection of 3× embryos at low frequency in mature *tgs1* seeds (i.e. < 1%). However, considering the defects reported during seed development, it is likely that the frequency of functional, unreduced female gametes is higher than that estimated in mature seeds.

Discussion

Previous experiments in *L. angustifolius* (Taylor *et al.*, 2021) and *P. notatum* (Siena *et al.*, 2014; Colono *et al.*, 2019) supported a
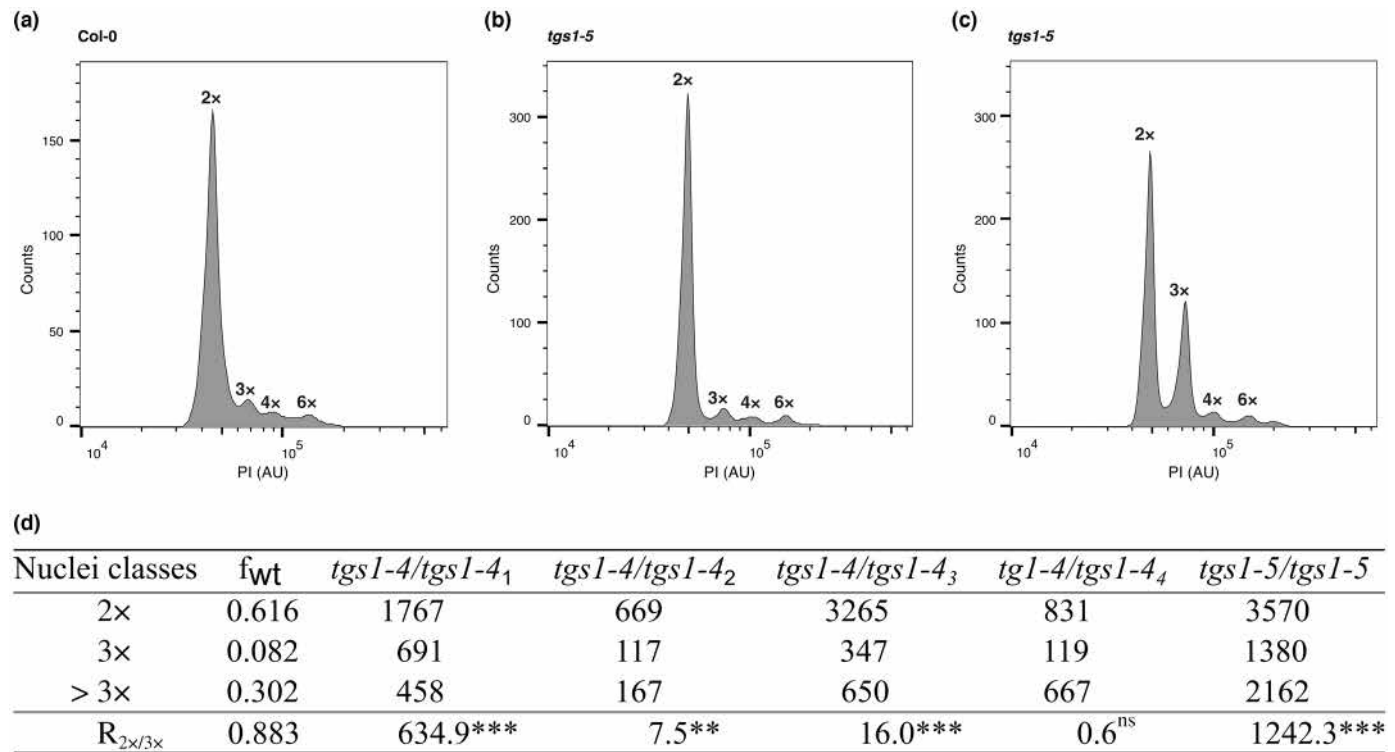

Fig. 6 DNA content analyses in WT and *tgs1* nuclei of *Arabidopsis thaliana* seeds. Distribution of signals for nuclei extracted from one bulk of four WT seeds (a), one bulk of four *tgs1-5* seeds with no evidence of 3× embryo (b), and one bulk of four *tgs1-5* seeds likely containing a 3× embryo (c). (d) Counts obtained for three classes of nuclei (2×, 3×, > 3×) from the five *tgs1* seed bulks showing significantly biased nuclei distributions compared with nuclei proportions in WT seeds (f_{WT}) estimated from 17 bulks (two-tailed *P* value for χ^2 (2, *n* = 950–7115) < 0.0001). $R_{2\times/3\times}$ shows χ^2 (1, *n* = 786–4950) values for testing 2×/3× nuclei ratios. ns, ** and *** denote two-tailed *P* values > 0.05, < 0.01, and < 0.001, respectively.

Nuclei classes	f_{WT}	*tgs1-4/tgs1-4*₁	*tgs1-4/tgs1-4*₂	*tgs1-4/tgs1-4*₃	*tg1-4/tgs1-4*₄	*tgs1-5/tgs1-5*
2×	0.616	1767	669	3265	831	3570
3×	0.082	691	117	347	119	1380
> 3×	0.302	458	167	650	667	2162
$R_{2\times/3\times}$	0.883	634.9***	7.5**	16.0***	0.6[ns]	1242.3***

role for TGS1 in plant development. However, the lack of biological resources and of molecular and cell biology tools in nonmodel species renders difficult the monitoring of expression patterns during reproduction and the investigation of reproductive cell identities and ploidy levels in apomictic and sexual relatives. Here, we used the *Arabidopsis* model to resolve in detail both expression patterns and mutant phenotypes.

Apospory could result from ectopic synchronicity of MMC and gametophytic cell fates

Our work indicates that the unique TGS1 yeast homolog conserved throughout plant evolution possesses a singular domain architecture combining the typical SAM domain of yeast TGS1, a WW domain and two N-terminal hydrophobic domains, suggesting that it fulfills essential functions for plant development. Indeed, our functional analyses in *Arabidopsis* revealed a role in canalizing cell fate specification during female sexual reproduction as *tgs1* mutations compromise the unicity of the cell specified for sporogenesis (MMC in the nucellus), gametophytic development (FM in the tetrad), and gametogenesis in the FG (egg cell). TGS1 depletion alters cell fate specification both in time and space as indicated, respectively, by ectopic acquisition of germline cell fate in nucellar enlarged MMC-like cell during meiosis, and the formation of more than one FM within tetrads and ectopic egg cell fate adoption in the egg apparatus. Numerous mutants affecting uniqueness and initiation of the female germline have been reported in Arabidopsis (e.g. Böwer & Schnittger, 2021). Among these, however, only mutations in components of the THO/TREX complex (i.e. *TRANSCRIPTION EXPORT1* or *TEX1*; Su *et al.*, 2017) and in the ATP-dependent RNA helicase *MNEME* (*MEM*; Schmidt *et al.*, 2011) also produce unreduced FGs from enlarged nucellar cells (and ectopically expressing a KNU reporter in *tex1* mutants). Therefore, together with *tex1* and *mem*, *tgs1* mutations produce phenotypes among the most closely resembling apospory in *Arabidopsis*, a claim well supported by the apospory-like phenotypes observed in *TGS1* RNAi transgenic lines of sexual *Paspalum* plants (Colono *et al.*, 2019). Interestingly, the pattern of ectopic *pKNU:nlsYFP* signals in enlarged MMC-like cells in *tgs1* ovules differs from that in *tex1* ovules and in many other mutants promoting ectopic MMC-like cells, while it remains unknown in *mem* ovules. In these mutants, signals are observed in adjacent enlarged cells before meiosis, whereas in *tgs1* mutants the ectopic *pKNU:nlsYFP* signals likely initiate at the end of meiosis as most positive, enlarged MMC-like cells were adjacent to a FM (Fig. 2l). However, although MMC-like cells in *mem* and *tex1* mutants can initiate gametophytic development without meiosis as revealed by the analysis of meiotic and gametophytic specific reporters (respectively, DMC1 immunolocalization in *tex1* and *pAKV:H2B-YFP*), *mem* unreduced FGs abort development and no evidence for functional, mature *tex1* FG has been reported. In contrast, the asynchronous *pKNU:nlsYFP* expression pattern in *tgs1* ovules strongly recalls the developmental course of unreduced FGs in aposporous plants, which typically initiates during meiosis in *Paspalum* and *Hieracium* (Koltunow *et al.*, 1998; Quarin *et al.*, 2001; Soliman

et al., 2021). In addition, our observations support the hypothesis of Juranić *et al.* (2018) for the requirement of a contact between aposporous initials and the FM to acquire gametophytic cell fate in *Hieracium* apomicts. The rare occurrence of extremely enlarged cell lacking both GFP signal and contact with the FM in *tgs1*/*pWOX2-CENH3-GFP* ovules (1/105; Fig. 2s) is consistent with such requirement. We could not resolve *pKNU:nlsYFP* and *pWOX2-CENH3-GFP* signals to a time scale nor characterize *tgs1* plants carrying both reporters, but they seem to be expressed at the same time in the precursor cells of unreduced gametophytes. Whether this results from cell–cell communication cues and ultimately contributes to establishing gametophytic development in MMC-like cells needs both to be confirmed. However, it is tempting to speculate a working model for asynchronous MMC specification in cells adjacent to a FM as a key event to establish apospory. Finally, although occurring at low frequency (*c.* 0.75%; 4 in 520 seeds), the formation of triploid embryos indicates that an alternative female germline lineage without meiosis can achieve viable seeds in *tgs1* mutants, an outcome that was not reported for the *tex1* and *mem* mutants.

TGS1, an integrator of female reproductive development?

Our observations indicate that TGS1 is strongly expressed in tissues harboring the cell selected during critical transitions throughout female germline development, including the ovule primordium where the archespore is specified (Fig. 1e); the proximal domain of the ovule that contains the megaspore surviving meiosis (Fig. 1i); and the egg cell in the FG (Fig. 1l,m). In contrast, developmental phases in between these key events show reduced expression levels (Fig. 1f–h and Fig. 1j,k for megasporogenesis and gametophyte development, respectively). This temporal pattern coincides well with that of specific cell fate reporters, such as KNU that appears early during ovule development in archesporial cells (Payne *et al.*, 2004), WOX2 for functional spore selection (Keçeli *et al.*, 2017), and egg cell reporters (*EC1:NLS_3xdsRed* in FGR7.0), and supports our hypothesis for a role of TGS1 in specifying reproductive cell types. At the onset of reproductive development, TGS1 pattern is somewhat reminiscent of that observed for regulators of cytokinin biosynthesis (e.g. ARABIDOPSIS HISTINE KINASE2-4/CYTOKININ RESPONSE1; Terceros *et al.*, 2020) and signaling (e.g. BEL1 and SPOROCYTELESS (SPL); Bencivenga *et al.*, 2012); the two AGAMOUS-related transcription factors, STK and SHATTERPROOF2 (Mizzotti *et al.*, 2014), and PEPPER (PEP) one member of their regulatory module (Rodríguez-Cazorla *et al.*, 2018); and cytochrome P450 KLUH (KLU; Adamski *et al.*, 2009). These proteins all participate in regulatory modules controlling either ovule patterning or cell fate specification in both the nucellus and the FG (Pinto *et al.*, 2019; Terceros *et al.*, 2020; Böwer & Schnittger, 2021). However, when depleted, they cause alternative phenotypes with respect to *tgs1* mutations (e.g. aberrant ovule patterning, nucellus cells prevented from adopting MMC fate, meiotic and FG arrest), except for *stk* mutations, which are responsible for the emergence of multiple enlarged cells in the nucellus through indirect SPL ectopic expression via the RdDM

pathway (Mendes *et al.*, 2020). How TGS1 mediates reproductive fate determination in the nucellus remains to be elucidated, but it is attractive to speculate whether TGS1 and STK belong to the same network acting during early steps of ovule primordium development, an assumption well supported by the regulation of *STK* by the HUA-PEP module, a complex of RNA-binding proteins responsible for pre-mRNA processing (Rodríguez-Cazorla *et al.*, 2018) and that could partner with TGS1 considering its activity in transcriptional regulation (Zhu *et al.*, 2001).

Abnormalities in FM specification at the end of meiosis appear somewhat different from that observed in *Arabidopsis* mutants affected in this process. In plants overexpressing ARABINO-GLUCAN PROTEIN18 (AGP18) and in the septuple *interactor/inhibitor of cyclin-dependent kinase* (*ick*) mutant, one to four megaspores at any position can survive, acquire FM fate and, eventually, produce a FG in *ick* mutants (Demesa-Arévalo & Vielle-Calzada, 2013; Cao *et al.*, 2018). In contrast, *tgs1* ovules typically contained tetrads with the two chalazal megaspores specified for gametophytic development (i.e. positive for pWOX2:CENH3:GFP; Fig. 2p) while the micropylar spores remained nonfunctional and degenerated. As shown by ICK inactivation, the micropylar cell of the meiotic dyad often undergoes an incomplete second meiotic division in Arabidopsis (Cao *et al.*, 2018), therefore suggesting that TGS1 repressing activity requires the completion of the second meiotic division.

Finally, TGS1 expression throughout coenocytic FG development was weak until we observed strong GFP signals in the egg cell (and to some extent in the central cell) after FG cellularization. This event marks cell fate acquisition in the *Arabidopsis* FG (Susaki *et al.*, 2021) and, likewise, our data suggest that adopting a strong, specific TGS1 expression level could also be a marker for egg cell fate. In support, nuclei misplacement and overproliferation, and dual cellular identities in micropylar end of *tgs1* FGs substantiate a role in coordinating gametophytic development and specifying cell fates in a manner reminiscent of AMP1, ATO, and RKD transcription factors, and of BEL1-LIKE HOMEODOMAIN1, whose depletion and ectopic expression in the *Arabidopsis* FG, respectively, result in egg cell fate in synergid cells (Pagnussat *et al.*, 2007; Moll *et al.*, 2008; Kong *et al.*, 2015; Tedeschi *et al.*, 2017). Gametic mis-specification did not prevent pollen guidance nor double fertilization, but seeds derived from *tgs1* FGs showed reduced viability (Table 1) and a variety of defects, including mixed cellular identities in fertilization products, abnormal embryo patterning, reduced proliferation in the endosperm, multiple zygote and embryo development. As paternal *TGS1* alleles do not rescue defects in *tgs1*/+ seeds (Table 1), these abnormal phenotypes likely resulted from adverse effects of mis-specification in the FG on the regulation of mechanisms mediating maternal gametophytic control on early seed development (i.e. transcript carryover, epigenetic reprogramming, cell cycle regulation, and hormonal signaling; Ge *et al.*, 2010; Dresselhaus & Jürgens, 2021; Verma *et al.*, 2022).

These findings, the versatile functions of TGS1 proteins in RNA biology and transcriptional regulation and, possibly, other unknown activities as suggested by the presence of the protein–protein interaction WW domain, posit RNA methyltransferases as attractive integrators of the epigenetic, hormonal, and cell cycle components controlling the female reproductive lineage in plants. The incomplete penetrance of the defects caused by the two *tgs1* mutations reported here likely reflects functional redundancy involving paralogous TGS1-LIKE genes or epistatic interactions involving unrelated, yet unknown genes. In regard to TGS1 regulatory function through splicing of genes required for sporogenesis in yeast (Qiu *et al.*, 2011), the critical role of alternative splicing in post-transcriptional regulation of genes essential to plant reproduction (Cucinotta *et al.*, 2021; H. Li *et al.*, 2021; Kashkan *et al.*, 2022) might require TGS1, a hypothesis we are currently examining through RNAseq in reproductive tissues of *A. thaliana*.

In conclusion, our work indicates that TGS1 contributes to the evolutionary acquisition of monospory (i.e. the formation of a single FG from the most chalazal spore), a dominant trait among angiosperms likely canalized toward the prevention of multiple female germline development (Webb & Gunning, 1990; Bachelier & Friedman, 2011). TGS1 depletion in *Arabidopsis* recapitulates, to varying degrees, the reproductive phenotypes unleashing the canalizing mechanisms that operate during female germline development and, in consequence, promotes favorable conditions for the emergence of an aposporous developmental pathway in a sexually reproducing species. Heterochrony plays an essential role in living organism diversification and has been essential for gametophyte development evolution (Buendía-Monreal & Gillmor, 2018). Here, we postulate that apospory may result from a heterochronic shift allowing MMC specification and gametophytic fate, two cellular decisions separated in time during female germline progression, to occur concurrently. Therefore, TGS1 appears to be a candidate for the genetic control of critical fate decisions that govern female germline development in plants. Our findings open the wedge for investigating how the interplay between TGS1 and key pathways for plant reproduction involved in small RNAs, phytohormones regulation, and cell–cell communication (Lora *et al.*, 2019; Pinto *et al.*, 2019; Petrella *et al.*, 2021) regulates cell fate decision during plant female reproduction.

Acknowledgements

New
Phytologist

Competing interests

None declared.

Author contributions

OL and LAS conceived and designed the study. BS, CM, JMV, LAS, MI and OL conducted the experiments. BS, CM, JMV, JPAO, LAS, MI, OL and SCP contributed to analyze the data. LAS, MI and OL prepared the figures. LAS and OL wrote the manuscript and BS, CM, JMV, JPAO, MI and SCP contributed to its revision and editing.

ORCID

Mathieu Ingouff (iD) https://orcid.org/0000-0002-6106-4564
Olivier Leblanc (iD) https://orcid.org/0000-0003-3641-1875
Caroline Michaud (iD) https://orcid.org/0000-0002-0620-2442
Juan Pablo A. Ortiz (iD) https://orcid.org/0000-0001-8460-6154
Silvina C. Pessino (iD) https://orcid.org/0000-0002-0200-8706
Benjamin Selles (iD) https://orcid.org/0000-0002-9260-9344
Lorena A. Siena (iD) https://orcid.org/0000-0003-3738-9075

Data availability

The data that support the findings of this study are available in the main text and figures and from Supporting Information.

References

Adamski NM, Anastasiou E, Eriksson S, O'Neill CM, Lenhard M. 2009. Local maternal control of seed size by KLUH/CYP78A5-dependent growth signaling. *Proceedings of the National Academy of Sciences, USA* 106: 20115–20120.

Autran D, Baroux C, Raissig MT, Lenormand T, Wittig M, Grob S, Steimer A, Barann M, Klostermeier UC, Leblanc O *et al.* 2011. Maternal epigenetic pathways control parental contributions to Arabidopsis early embryogenesis. *Cell* 145: 707–719.

Bachelier JB, Friedman WE. 2011. Female gamete competition in an ancient angiosperm lineage. *Proceedings of the National Academy of Sciences, USA* 108: 12360–12365.

Barcaccia G, Palumbo F, Sgorbati S, Albertini E, Pupilli F. 2020. A reappraisal of the evolutionary and developmental pathway of apomixis and its genetic control in angiosperms. *Genes* 11: 859.

Bencivenga S, Simonini S, Benková E, Colombo L. 2012. The transcription factors BEL1 and SPL are required for cytokinin and auxin signaling during ovule development in Arabidopsis. *Plant Cell* 24: 2886–2897.

Böwer F, Schnittger A. 2021. How to switch from mitosis to meiosis: regulation of germline entry in plants. *Annual Review of Genetics* 55: 427–452.

Bowman JL, Sakakibara K, Furumizu C, Dierschke T. 2016. Evolution in the cycles of life. *Annual Review of Genetics* 50: 133–154.

Brukhin V, Baskar R. 2019. A brief note on genes that trigger components of apomixis. *Journal of Biosciences* 44: 45.

Buendía-Monreal M, Gillmor CS. 2018. The times they are A-Changin': heterochrony in plant development and evolution. *Frontiers in Plant Science* 9: 1349.

Cai H, Liu L, Huang Y, Zhu W, Qi J, Xi X, Aslam M, Dresselhaus T, Qin Y. 2022. Brassinosteroid signaling regulates female germline specification in Arabidopsis. *Current Biology* 32: 1102–1114.

Cao L, Wang S, Venglat P, Zhao L, Cheng Y, Ye S, Qin Y, Datla R, Zhou Y, Wang H. 2018. Arabidopsis ICK/KRP cyclin-dependent kinase inhibitors function to ensure the formation of one megaspore mother cell and one functional megaspore per ovule. *PLoS Genetics* 14: e1007230.

Chen L, Roake CM, Galati A, Bavasso F, Micheli E, Saggio I, Schoeftner S, Cacchione S, Gatti M, Artandi SE *et al.* 2020. Loss of human TGS1 hypermethylase promotes increased telomerase RNA and telomere elongation. *Cell Reports* 30: 1358–1372.

Cheng L, Zhang Y, Zhang Y, Chen T, Xu Y-Z, Rong YS. 2020. Loss of the RNA trimethylguanosine cap is compatible with nuclear accumulation of spliceosomal snRNAs but not pre-mRNA splicing or snRNA processing during animal development. *PLoS Genetics* 16: e1009098.

Cole M, Chandler J, Weijers D, Jacobs B, Comelli P, Werr W. 2009. DORNRÖSCHEN is a direct target of the auxin response factor MONOPTEROS in the Arabidopsis embryo. *Development* 136: 1643–1651.

Colono C, Ortiz JPA, Permingeat HR, Souza Canada ED, Siena LA, Spoto N, Galdeano F, Espinoza F, Leblanc O, Pessino SC. 2019. A plant-specific TGS1 homolog influences gametophyte development in sexual tetraploid *Paspalum notatum* ovules. *Frontiers in Plant Science* 10: 1566.

Conner JA, Mookkan M, Huo H, Chae K, Ozias-Akins P. 2015. A parthenogenesis gene of apomict origin elicits embryo formation from unfertilized eggs in a sexual plant. *Proceedings of the National Academy of Sciences, USA* 112: 11205–11210.

Conner JA, Podio M, Ozias-Akins P. 2017. Haploid embryo production in rice and maize induced by PsASGR-BBML transgenes. *Plant Reproduction* 30: 41–52.

Corral JM, Vogel H, Aliyu OM, Hensel G, Thiel T, Kumlehn J, Sharbel TF. 2013. A conserved apomixis-specific polymorphism is correlated with exclusive exonuclease expression in premeiotic ovules of apomictic *Boechera* species1[W] [OPEN]. *Plant Physiology* 163: 1660–1672.

Cucinotta M, Cavalleri A, Guazzotti A, Astori C, Manrique S, Bombarely A, Oliveto S, Biffo S, Weijers D, Kater MM *et al.* 2021. Alternative splicing generates a MONOPTEROS isoform required for ovule development. *Current Biology* 31: 892–899.

Demesa-Arévalo E, Vielle-Calzada J-P. 2013. The classical Arabinogalactan protein AGP18 mediates megaspore selection in Arabidopsis. *Plant Cell* 25: 1274–1287.

Dierschke T, Flores-Sandoval E, Rast-Somssich MI, Althoff F, Zachgo S, Bowman JL. 2021. Gamete expression of TALE class HD genes activates the diploid sporophyte program in *Marchantia polymorpha. eLife* 10: e57088.

Dresselhaus T, Jürgens G. 2021. Comparative embryogenesis in angiosperms: activation and patterning of embryonic cell lineages. *Annual Review of Plant Biology* 72: 641–676.

Galla G, Basso A, Grisan S, Bellucci M, Pupilli F, Barcaccia G. 2019. Ovule gene expression analysis in sexual and aposporous apomictic *Hypericum perforatum* L. (Hypericaceae) accessions. *Frontiers in Plant Science* 10: 654.

Gao J, Wallis JG, Jewell JB, Browse J. 2017. Trimethylguanosine Synthase1 (TGS1) is essential for chilling tolerance. *Plant Physiology* 174: 1713–1727.

Ge X, Chang F, Ma H. 2010. Signaling and transcriptional control of reproductive development in Arabidopsis. *Current Biology* 20: R988–R997.

Gietz RD, Schiestl RH. 2007. High-efficiency yeast transformation using the LiAc/SS carrier DNA/PEG method. *Nature Protocols* 2: 31–34.

Grimanelli D. 2012. Epigenetic regulation of reproductive development and the emergence of apomixis in angiosperms. *Current Opinion in Plant Biology* 15: 57–62.

Hater F, Nakel T, Groß-Hardt R. 2020. Reproductive multitasking: the female gametophyte. *Annual Review of Plant Biology* 71: 517–546.

Hausmann S, Zheng S, Costanzo M, Brost RL, Garcin D, Boone C, Shuman S, Schwer B. 2008. Genetic and biochemical analysis of yeast and human cap trimethylguanosine synthase. *Journal of Biological Chemistry* 283: 31706–31718.

Hisanaga T, Yamaoka S, Kawashima T, Higo A, Nakajima K, Araki T, Kohchi T, Berger F. 2019. Building new insights in plant gametogenesis from an evolutionary perspective. *Nature Plants* 5: 663–669.

Huang J, Zhao L, Malik S, Gentile BR, Xiong V, Arazi T, Owen HA, Friml J, Zhao D. 2022. Specification of female germline by microRNA orchestrated auxin signaling in Arabidopsis. *Nature Communications* 13: 6960.

Jia Y, Viswakarma N, Crawford SE, Sarkar J, Sambasiva Rao M, Karpus WJ, Kanwar YS, Zhu Y-J, Reddy JK. 2012. Early embryonic lethality of mice with disrupted transcription cofactor PIMT/NCOA6IP/Tgs1 gene. *Mechanisms of Development* 129: 193–207.

Juranić M, Tucker MR, Schultz CJ, Shirley NJ, Taylor JM, Spriggs A, Johnson SD, Bulone V, Koltunow AM. 2018. Asexual female gametogenesis involves contact with a sexually-fated megaspore in *Apomictic hieracium. Plant Physiology* 177: 1027–1049.

Kashkan I, Hrtyan M, Retzer K, Humpolíčková J, Jayasree A, Filepová R, Vondráková Z, Simon S, Rombaut D, Jacobs TB et al. 2022. Mutually opposing activity of PIN7 splicing isoforms is required for auxin-mediated tropic responses in Arabidopsis thaliana. *New Phytologist* 233: 329–343.

Keçeli BN, De Storme N, Geelen D. 2017. *In vivo* ploidy determination of arabidopsis thaliana male and female gametophytes. In: Schmidt A, ed. *Methods in molecular biology. plant germline development.* New York, NY, USA: Springer New York, 77–85.

Khanday I, Skinner D, Yang B, Mercier R, Sundaresan V. 2019. A male-expressed rice embryogenic trigger redirected for asexual propagation through seeds. *Nature* 565: 91–95.

Khanday I, Sundaresan V. 2021. Plant zygote development: recent insights and applications to clonal seeds. *Current Opinion in Plant Biology* 59: 101993.

Kim S, Park J-S, Lee J, Lee KK, Park O-S, Choi H-S, Seo PJ, Cho H-T, Frost JM, Fischer RL et al. 2021. The DME demethylase regulates sporophyte gene expression, cell proliferation, differentiation, and meristem resurrection. *Proceedings of the National Academy of Sciences, USA* 118: e2026806118.

Koltunow AM, Johnson SD, Bicknell RA. 1998. Sexual and apomictic development in Hieracium. *Sexual Plant Reproduction* 11: 213–230.

Koltunow AMG, Johnson SD, Rodrigues JCM, Okada T, Hu Y, Tsuchiya T, Wilson S, Fletcher P, Ito K, Suzuki G et al. 2011. Sexual reproduction is the default mode in apomictic *Hieracium* subgenus *Pilosella*, in which two dominant loci function to enable apomixis. *The Plant Journal* 66: 890–902.

Komonyi O, Pápai G, Enunlu I, Muratoglu S, Pankotai T, Kopitova D, Maróy P, Udvardy A, Boros I. 2005. DTL, the Drosophila homolog of PIMT/Tgs1 nuclear receptor coactivator-interacting protein/RNA methyltransferase, has an essential role in development. *Journal of Biological Chemistry* 280: 12397–12404.

Kong J, Lau S, Jürgens G. 2015. Twin plants from supernumerary egg cells in Arabidopsis. *Current Biology* 25: 225–230.

Lemm I, Girard C, Kuhn AN, Watkins NJ, Schneider M, Bordonné R, Lührmann R. 2006. Ongoing U snRNP biogenesis is required for the integrity of Cajal bodies. *Molecular Biology of the Cell* 17: 3221–3231.

León-Martínez G, Vielle-Calzada J-P. 2019. Apomixis in flowering plants: developmental and evolutionary considerations. *Current Topics in Developmental Biology* 131: 565–604.

Li H, Li A, Shen W, Ye N, Wang G, Zhang J. 2021. Global survey of alternative splicing in rice by direct RNA sequencing during reproductive development: landscape and genetic regulation. *Rice* 14: 75.

Li Y, Lin Z, Yue Y, Zhao H, Fei XEL, Liu C, Chen S, Lai J, Song W. 2021. Loss-of-function alleles of ZmPLD3 cause haploid induction in maize. *Nature Plants* 7: 1579–1588.

Lora J, Yang X, Tucker MR. 2019. Establishing a framework for female germline initiation in the plant ovule. *Journal of Experimental Botany* 70: 2937–2949.

Mancini M, Permingeat H, Colono C, Siena L, Pupilli F, Azzaro C, de Alencar Dusi DM, de Campos Carneiro VT, Podio M, Seijo JG et al. 2018. The MAP3K-coding QUI-GON JINN (QGJ) gene is essential to the formation of unreduced embryo sacs in *Paspalum. Frontiers in Plant Science* 9: 1547.

Martinez I, Hayes KE, Barr JA, Harold AD, Xie M, Bukhari SIA, Vasudevan S, Steitz JA, DiMaio D. 2017. An Exportin-1–dependent microRNA biogenesis pathway during human cell quiescence. *Proceedings of the National Academy of Sciences, USA* 114: E4961–E4970.

Matzk F, Meister A, Schubert I. 2000. An efficient screen for reproductive pathways using mature seeds of monocots and dicots. *The Plant Journal* 21: 97–108.

Mendes MA, Petrella R, Cucinotta M, Vignati E, Gatti S, Pinto SC, Bird DC, Gregis V, Dickinson H, Tucker MR et al. 2020. The RNA-dependent DNA methylation pathway is required to restrict SPOROCYTELESS/NOZZLE expression to specify a single female germ cell precursor in Arabidopsis. *Development* 147: dev194274.

Mizzotti C, Ezquer I, Paolo D, Rueda-Romero P, Guerra RF, Battaglia R, Rogachev I, Aharoni A, Kater MM, Caporali E et al. 2014. SEEDSTICK is a master regulator of development and metabolism in the Arabidopsis seed coat. *PLoS Genetics* 10: e1004856.

Moll C, Nielsen N, Groß-Hardt R. 2008. Mutants with aberrant numbers of gametic cells shed new light on old questions. *Plant Biology* 10: 529–533.

Mosquna A, Katz A, Decker EL, Rensing SA, Reski R, Ohad N. 2009. Regulation of stem cell maintenance by the Polycomb protein FIE has been conserved during land plant evolution. *Development* 136: 2433–2444.

Mouaikel J, Bujnicki JM, Tazi J, Bordonné R. 2003. Sequence-structure-function relationships of Tgs1, the yeast snRNA/snoRNA cap hypermethylase. *Nucleic Acids Research* 31: 4899–4909.

Mouaikel J, Verheggen C, Bertrand E, Tazi J, Bordonné R. 2002. Hypermethylation of the cap structure of both yeast snRNAs and snoRNAs requires a conserved methyltransferase that is localized to the nucleolus. *Molecular Cell* 9: 891–901.

Nakajima K. 2018. Be my baby: patterning toward plant germ cells. *Current Opinion in Plant Biology* 41: 110–115.

One Thousand Plant Transcriptomes Initiative. 2019. One thousand plant transcriptomes and the phylogenomics of green plants. *Nature* 574: 679–685.

Ozias-Akins P, Conner JA. 2020. Clonal reproduction through seeds in sight for crops. *Trends in Genetics* 36: 215–226.

Pagnussat GC, Yu H-J, Sundaresan V. 2007. Cell-fate switch of synergid to egg cell in Arabidopsis eostre mutant embryo sacs arises from misexpression of the BEL1-like homeodomain gene BLH1. *Plant Cell* 19: 3578–3592.

Pandey S, Moradi AB, Dovzhenko O, Touraev A, Palme K, Welsch R. 2022. Molecular control of sporophyte-gametophyte ontogeny and transition in plants. *Frontiers in Plant Science* 12: 789789.

Payne T, Johnson SD, Koltunow AM. 2004. KNUCKLES (KNU) encodes a C2H2 zinc-finger protein that regulates development of basal pattern elements of the Arabidopsis gynoecium. *Development* 131: 3737–3749.

Petrella R, Cucinotta M, Mendes MA, Underwood CJ, Colombo L. 2021. The emerging role of small RNAs in ovule development, a kind of magic. *Plant Reproduction* 34: 335–351.

Petrella R, Gabrieli F, Cavalleri A, Schneitz K, Colombo L, Cucinotta M. 2022. Pivotal role of STIP in ovule pattern formation and female germline development in *Arabidopsis thaliana. Development* 149: dev201184.

Pinto SC, Mendes MA, Coimbra S, Tucker MR. 2019. Revisiting the female germline and its expanding toolbox. *Trends in Plant Science* 24: 455–467.

Qiu ZR, Shuman S, Schwer B. 2011. An essential role for trimethylguanosine RNA caps in Saccharomyces cerevisiae meiosis and their requirement for splicing of SAE3 and PCH2 meiotic pre-mRNAs. *Nucleic Acids Research* 39: 5633–5646.

Quarin CL, Espinoza F, Martinez EJ, Pessino SC, Bovo OA. 2001. A rise of ploidy level induces the expression of apomixis in *Paspalum notatum. Sexual Plant Reproduction* 13: 243–249.

Rodríguez-Cazorla E, Ortuño-Miquel S, Candela H, Bailey-Steinitz LJ, Yanofsky MF, Martínez-Laborda A, Ripoll J-J, Vera A. 2018. Ovule identity mediated by pre-mRNA processing in Arabidopsis. *PLoS Genetics* 14: e1007182.

Sakakibara K, Ando S, Yip HK, Tamada Y, Hiwatashi Y, Murata T, Deguchi H, Hasebe M, Bowman JL. 2013. KNOX2 genes regulate the haploid-to-diploid morphological transition in land plants. *Science* 339: 1067–1070.

Sanchez-Vera V, Landberg K, Lopez-Obando M, Thelander M, Lagercrantz U, Muñoz-Viana R, Schmidt A, Grossniklaus U, Sundberg E. 2022. The *Physcomitrium patens* egg cell expresses several distinct epigenetic components and utilizes homologues of BONOBO genes for cell specification. *New Phytologist* 233: 2614–2628.

Schmidt A. 2020. Controlling apomixis: shared features and distinct characteristics of gene regulation. *Genes* 11: 329.

Schmidt A, Schmid MW, Grossniklaus U. 2015. Plant germline formation: common concepts and developmental flexibility in sexual and asexual reproduction. *Development* **142**: 229–241.

Schmidt A, Wuest SE, Vijverberg K, Baroux C, Kleen D, Grossniklaus U. 2011. Transcriptome analysis of the Arabidopsis megaspore mother cell uncovers the importance of RNA helicases for plant germline development. *PLoS Biology* **9**: e1001155.

Selva JP, Siena L, Rodrigo JM, Garbus I, Zappacosta D, Romero JR, Ortiz JPA, Pessino SC, Leblanc O, Echenique V. 2017. Temporal and spatial expression of genes involved in DNA methylation during reproductive development of sexual and apomictic *Eragrostis curvula*. *Scientific Reports* **7**: 15092.

Siena LA, Ortiz JPA, Leblanc O, Pessino S. 2014. PnTgs1-like expression during reproductive development supports a role for RNA methyltransferases in the aposporous pathway. *BMC Plant Biology* **14**: 297.

Soliman M, Podio M, Marconi G, Di Marsico M, Ortiz JPA, Albertini E, Delgado L. 2021. Differential epigenetic marks are associated with apospory expressivity in diploid hybrids of *Paspalum rufum*. *Plants* **10**: 793.

Su Z, Zhao L, Zhao Y, Li S, Won S, Cai H, Wang L, Li Z, Chen P, Qin Y *et al.* 2017. The THO complex non-cell-autonomously represses female germline specification through the TAS3-ARF3 module. *Current Biology* **27**: 1597–1609.

Sudol M. 1996. Structure and function of the WW domain. *Progress in Biophysics and Molecular Biology* **65**: 113–132.

Susaki D, Suzuki T, Maruyama D, Ueda M, Higashiyama T, Kurihara D. 2021. Dynamics of the cell fate specifications during female gametophyte development in Arabidopsis. *PLoS Biology* **19**: e3001123.

Taylor CM, Garg G, Berger JD, Ribalta FM, Croser JS, Singh KB, Cowling WA, Kamphuis LG, Nelson MN. 2021. A Trimethylguanosine Synthase1-like (TGS1) homologue is implicated in vernalisation and flowering time control. *Theoretical and Applied Genetics* **134**: 3411–3426.

Tedeschi F, Rizzo P, Rutten T, Altschmied L, Bäumlein H. 2017. RWP-RK domain-containing transcription factors control cell differentiation during female gametophyte development in Arabidopsis. *New Phytologist* **213**: 1909–1924.

Terceros GC, Resentini F, Cucinotta M, Manrique S, Colombo L, Mendes MA. 2020. The importance of cytokinins during reproductive development in Arabidopsis and beyond. *International Journal of Molecular Sciences* **21**: E8161.

Underwood CJ, Vijverberg K, Rigola D, Okamoto S, Oplaat C, Den Camp RHMO, Radoeva T, Schauer SE, Fierens J, Jansen K *et al.* 2022. A PARTHENOGENESIS allele from apomictic dandelion can induce egg cell division without fertilization in lettuce. *Nature Genetics* **54**: 84–93.

Verheggen C, Bertrand E. 2012. CRM1 plays a nuclear role in transporting snoRNPs to nucleoli in higher eukaryotes. *Nucleus* **3**: 132–137.

Verma S, Attuluri VPS, Robert HS. 2022. Transcriptional control of Arabidopsis seed development. *Planta* **255**: 90.

Vigneau J, Borg M. 2021. The epigenetic origin of life history transitions in plants and algae. *Plant Reproduction* **34**: 267–285.

Völz R, Heydlauff J, Ripper D, von Lyncker L, Groß-Hardt R. 2013. Ethylene signaling is required for synergid degeneration and the establishment of a pollen tube block. *Developmental Cell* **25**: 310–316.

Webb MC, Gunning BES. 1990. Embryo sac development in *Arabidopsis thaliana*. *Sexual Plant Reproduction* **3**: 244–256.

Wurth L, Gribling-Burrer A-S, Verheggen C, Leichter M, Takeuchi A, Baudrey S, Martin F, Krol A, Bertrand E, Allmang C. 2014. Hypermethylated-capped selenoprotein mRNAs in mammals. *Nucleic Acids Research* **42**: 8663–8677.

Yu H, Tsuchida M, Ando M, Hashizaki T, Shimada A, Takahata S, Murakami Y. 2021. Trimethylguanosine synthase 1 (Tgs1) is involved in Swi6/HP1-independent siRNA production and establishment of heterochromatin in fission yeast. *Genes to Cells* **26**: 203–218.

Zhu Y, Qi C, Cao W-Q, Yeldandi AV, Rao MS, Reddy JK. 2001. Cloning and characterization of PIMT, a protein with a methyltransferase domain, which interacts with and enhances nuclear receptor coactivator PRIP function. *Proceedings of the National Academy of Sciences, USA* **98**: 10380–10385.

Supporting Information

Additional Supporting Information may be found online in the Supporting Information section at the end of the article.

Fig. S1 Characterization of *Arabidopsis thaliana* T-DNA insertion lines for *At1g45231*.

Fig. S2 Multiple sequence alignment of plant proteins homologous to yeast TGS1.

Fig. S3 Detailed phylogenetic tree of Fig. 1(c).

Fig. S4 GUS patterns in reproductive tissues of *Arabidopsis thaliana* plants carrying *pAtTGS1:AtTGS1-GUS*.

Fig. S5 Formation of binucleated female gametophyte in *tgs1* ovules at meiosis in *Arabidopsis thaliana*.

Fig. S6 *pWOX2-CENH3-GFP* expression patterns during reproductive development in *Arabidopsis thaliana*.

Fig. S7 Identity defects in *tgs1* gametophytes in *Arabidopsis thaliana*.

Fig. S8 Phenotypes of *tgs1* embryos and germinated *tgs1* seedlings in *Arabidopsis thaliana*.

Notes S1 Multiple alignment of plant TGS1 proteins. This file opens in a text editor or using the MView utility.

Notes S2 Amino acid sequences of conversed blocks used for phylogenic tree inferences. This file opens in a text editor or using the MView utility.

Table S1 Sequences orthologous to yeast TGS1 by species.

Table S2 List of primers.

Please note: Wiley is not responsible for the content or functionality of any Supporting Information supplied by the authors. Any queries (other than missing material) should be directed to the *New Phytologist* Central Office.